Prospects of Discovery for Supersymmetry at the Tevatron

Teruki Kamon*
e-mail: t-kamon@tamu.edu
Department of Physics, Texas A&M University
College Station TX 77843-4242, USA

Abstract

We summarize a discovery potential for supersymmetric particles at the $p\overline{p}$ collider of Tevatron with center-of-mass energy $\sqrt{s} = 2$ TeV and integrated luminosity $\int \mathcal{L}\, dt$ = 15-30 fb^{-1}. Any direct search is kinematically limited to below 450 GeV/c^2. We, however, have a unique opportunity to test various supersymmetric scenarios by a measurement of the branching ratio for the rare decay mode $B_s \to \mu^+\mu^-$. Using the background estimate in the CDF analysis of $B_s \to \mu^+\mu^-$ in Run I, we investigate the prospects for studying this mode in Run II. CDF would be sensitive to this decay for a branching ratio $> 1.2 \times 10^{-8}$ with 15 fb^{-1} (or, if a similar analysis holds for DØ, $> 6.5 \times 10^{-9}$ for the combined data). For $\tan\beta > 30$, the $B_s \to \mu^+\mu^-$ search can probe the SUSY parameter space that cannot be probed by direct production of SUSY particles at Run II. An observation of $B_s \to \mu^+\mu^-$ with a large branching ratio $> 7(14) \times 10^{-8}$ (feasible with only 2 fb^{-1}) would be sufficient to exclude the mSUGRA model for $\tan\beta \leq 50(55)$ including other experimental constraints. For some models, the branching ratio can be large enough to be detected even for small $\tan\beta$ and large $m_{1/2}$.

1 Introduction

The Fermilab Tevatron collider will define the high energy frontier of particle physics while CERN's Large Hadron Collider is being built. The first stage (Run IIa) of the Tevatron collider Run II (March 2001-2005) will deliver at least 2 fb^{-1} of integrated luminosity per experiment at $\sqrt{s} = 2$ TeV. Major upgrades of the CDF and DØ detectors [1, 2] have been completed and we have being taking data. In the second stage

*Representing the CDF and DØ Collaborations. Plenary talk at 10th International Conference on Supersymmetry and Unification of Fundamental Interactions (SUSY02), June 17-23, 2002, DESY, Hamburg, Germany

(Run IIb) of Run II (starting in 2006), we expect 15 fb^{-1} of integrated luminosity per experiment at 2 TeV. Further upgrades of the two detectors are been undertaken.

Among various features, the detectors have the ability to trigger on displaced vertices from bottom and charm decays using a precise microvertex detector to enhance the Higgs search and the physics with top quarks. Searches for supersymmetry (SUSY) are among the main priorities along with Higgs and top physics for Run II.

Supersymmetry uniquely opens the possibility to directly connect the Standard Model (SM) with an ultimate unification of the fundamental interactions. With the results on electroweak and strong gauge couplings from CERN's e^+e^- collider LEP experiments and the top quark mass at CDF and DØ at the Tevatron, the models of SUSY have become more predictive and require a spectrum of new particles below a few TeV/c^2. Thus SUSY represents a natural candidate for the new physics expected to occur in the TeV energy domain.

In this paper, we summarize the prospects of SUSY searches/discovery either directly through collider processes or indirectly through rare processes at the Tevatron.

2 SUSY Models

One of the difficulties in determining predictions of generic Minimal Supersymmetric Standard Model (MSSM) lies in the large number of new parameters (over 100 free parameters) the theory implies. One may consider a theoretical framework to reduce the number of free parameters.

Fortunately SUSY models apply to a large number of different accelerator and cosmological phenomena, and a great deal of effort has been involved in recent years to use the data to limit the parameter space. Part of the difficulty in doing this resides in the success of the model in not disturbing the excellent agreement of the precision tests of the SM [3] due to the SUSY decoupling theorems which suppress SUSY contributions at low energies. Historically, the absence of flavor changing neutral currents at the tree level played an important role in the construction of the SM. They represent therefore an important class of phenomena that might show the presence of new physics, since the SM and the SUSY contributions contribute first at the loop level with comparable size. Thus the decay $b \to s\gamma$ has been a powerful tool in limiting the SUSY parameter space.

Extensive Monte Carlo (MC) studies were carried out during 1998 on the following four topics to maximize the direct SUSY/Higgs searches in Run II: (i) supergravity (SUGRA) [4], (ii) Gauge-mediated SUSY Breaking (GMSB) [5], (iii) beyond the MSSM [6], and (iv) Higgs [7]. The readers can refer to Ref. [8] for a summary of Run I SUSY searches. Among the experimental aspects, we conclude that it is important to have excellent triggering/tagging and identification for b's, τ's, γ's as well as e's and μ's. Thus we develop (A) low p_T lepton+track trigger, where the "track" object can be electron, muon, or hadronically decaying τ-lepton, (B1) $\geq$2-jets trigger + $\not\!\!E_T$ (> 25 GeV) and (B2) $\geq$2-jets trigger + $\not\!\!E_T$ (> 20 GeV with b/c tagging), instead of inclusive $\not\!\!E_T$ trigger, (C) better trigger/identification for prompt/displaced photons. Trigger B1 is extremely useful for reliable parametrization of high $\not\!\!E_T$ distribution due

to QCD events to reduce the systematic uncertainty [4].

We first consider minimal SUGRA (mSUGRA) and GMSB frameworks as examples of direct searches for SUSY production, which characterize the experimental triggers and analyses in b's, τ's, γ's. Details of all SUSY models and experimental prospects can be found in Refs. [4, 5, 6]. We then take the decay $B_s \to \mu^+\mu^-$ as an example of powerful tool in limiting SUSY parameter space at the Tevatron.

3 Direct Searches

3.1 Testing mSUGRA

The mSUGRA model [9, 10] depends on four parameters: m_0 (the universal scalar mass at M_G), $m_{1/2}$ (the universal gaugino mass at M_G), A_0 (the universal cubic soft breaking mass at M_G), and $\tan\beta$ (the ratio of two SUSY Higgs vacuum expectation values at the electroweak scale). In addition, the sign of μ (the Higgs mixing parameter) is arbitrary. With R parity invariance, the lightest neutralino ($\tilde{\chi}_1^0$) is assumed to be the lightest supersymmetric particle (LSP) and it is bino-like and stable. The $\tilde{\chi}_1^0$ then would pass through the detector without interaction. We fix $A_0 = 0$ and the sign of μ to be positive for simplicity, otherwise stated. Here the ISAJET sign convention for μ is used.

3.1.1 Chargino-Neutralino Associated Production

The trilepton signal arises when both the lightest chargino ($\tilde{\chi}_1^\pm$) and the next-to-lightest neutralino ($\tilde{\chi}_2^0$) decay leptonically in $p\overline{p} \to \tilde{\chi}_1^\pm \tilde{\chi}_2^0 + X$. An initial study of the final state of trilepton ($\ell\ell\ell$) plus $\not\!\!E_T$ for high luminosity ($\gtrsim$10 fb^{-1}) at the Tevatron was made in Ref. [11] for direct $\tilde{\chi}_1^\pm \tilde{\chi}_2^0$ production. Here $\ell\ell\ell = eee, ee\mu, e\mu\mu, \mu\mu\mu$ by excluding electron or muon from tau (τ) lepton leptonic decay. Further studies were also made for $p\overline{p} \to 3\ell + X$, including all SUSY production processes (*e.g.*, $\tilde{\ell}\tilde{\nu}$) and its decays [12, 13, 14, 4, 15]. Electron or muon from the leptonic decay mode of τ lepton were accepted. This requires CDF and DØ experiments to trigger and identify the leptons with low p_T ($\gtrsim$10 GeV/c). They also improved the SM background calculations including effects from W^*, Z^*, and γ^*.

The studies in Refs. [12, 14, 4, 15] have included hadronically decaying τ lepton as well. This requires both experiments to trigger and identify the τ leptons with low p_T ($\gtrsim$10 GeV/c). With high luminosity in Run II, an inclusive lepton trigger becomes more difficult because of such a large trigger rate. Thus a generic dilepton trigger, namely lepton + track trigger, is necessary [4].

In those studies, the final states of $3\ell + \not\!\!E_T$, $\ell^\pm\ell^\pm + \tau_h + \not\!\!E_T$ are found to be the best channels for the study of chargino-neutralino associated production. Trigger A, mentioned earlier, will play a key role to maximize the experimental sensitivity in this channels. Figure 1 shows 5σ discovery reach in the trilepton channel in mSUGRA for small $\tan\beta = 5$ and large $\tan\beta = 50$. We will be sensitive upto $m_{1/2} \simeq 250$ GeV/c^2 if $m_0 \lesssim 200$ GeV/c^2 and low $\tan\beta$ (*e.g.*, 5). With large $\tan\beta$ (*e.g.*, 50), upto $m_{1/2} \simeq 200$ GeV/c^2 if $m_0 \gtrsim 500$ GeV/c^2. It should be noted that the

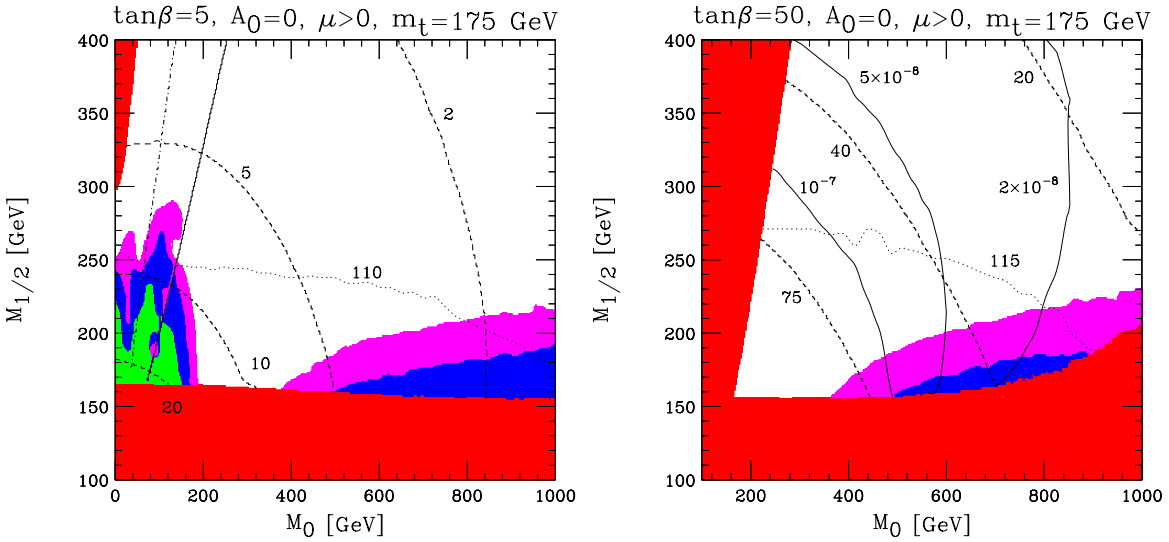

Figure 1: Regions of the $m_{1/2}$-m_0 plane where the trilepton events should be detectable at a level of 5σ significance for $\tan\beta = 5$ (left) and $\tan\beta = 50$ (right) [15]. Three areas are shown for an integrated luminosity of 30 fb^{-1} (magenta), 10 fb^{-1} (blue) and 2 fb^{-1} (green) and from top to bottom, respectively. The large red regions are excluded by theory and experiment. Dashed lines represent the SUSY contribution to the muon anomalous magnetic moment (in units of 10^{-10}) and the dotted lines are iso-mass contours of the lightest neutral Higgs boson. The solid contour (only for $\tan\beta = 50$) indicates the prediction for the branching ratio $Br[B_s \to \mu^+\mu^-]$. In the left ($\tan\beta = 5$) plot the solid line indicates where $M_{\tilde{\chi}_1^\pm} = M_{\tilde{\tau}_1}$ and the dot-dashed line $M_{\tilde{\chi}_1^\pm} = M_{\tilde{\nu}_\tau}$.

CDF and DØ analyses [16, 17] of the trilepton channel in Run I (about 100 pb^{-1}) were limited to $\tan\beta = 2$, $\mu < 0$ within the MSSM framework. The chargino mass upto about 80 GeV/c^2 ($m_{1/2}$ = 75 GeV/c^2) was excluded for $\tan\beta = 2$, $\mu < 0$ and $A_0 = 0$ if $M_{\tilde{q}} = M_{\tilde{g}}$ within mSUGRA [18].

3.1.2 Gluinos and Squarks Production

Gluinos ($\tilde{g}$) and squarks ($\tilde{q}$) are pair-produced at the Tevatron. Within the mSUGRA framework, $M_{\tilde{q}} \gtrsim 0.85\ M_{\tilde{g}}$. Thus, there appear two representative parameter regions in terms of the production: (i) $\tilde{g}\tilde{g}, \tilde{g}\tilde{q}$, and $\tilde{q}\bar{\tilde{q}}$ productions where $M_{\tilde{q}} \simeq M_{\tilde{g}}$ and (ii) $\tilde{g}\tilde{g}$ production where $M_{\tilde{q}} \gg M_{\tilde{g}}$.

In most of the parameter space accessible at the Tevatron, the left-chiral squark dominantly decays into a quark and either a $\tilde{\chi}_1^\pm$ or a $\tilde{\chi}_2^0$. Those branching ratios are $B(\tilde{q}_L \to q'\tilde{\chi}_1^\pm) \simeq 65\%$ and $B(\tilde{q}_L \to q\tilde{\chi}_2^0) \simeq 30\%$. Since $M_{\tilde{q}} - M_{\tilde{\chi}_1^\pm} > M_{\tilde{\chi}_1^\pm} - M_{\tilde{\chi}_1^0}$, the jet in the $\tilde{q}_L \to q'\tilde{\chi}_1^\pm$ (or $\tilde{q}_L \to q\tilde{\chi}_2^0$) decay likely has larger E_T than those in the $\tilde{\chi}_1^\pm \to q\bar{q}'\tilde{\chi}_1^0$ (or $\tilde{\chi}_2^0 \to qq'\tilde{\chi}_1^0$) decay [19]. Similarly, at least one jet in the gluino decay ($\tilde{g} \to q\bar{q}'\tilde{\chi}_1^\pm$ or $q\bar{q}\tilde{\chi}_2^0$ through a real of virtual squark) has large E_T. Thus, pair-produced squarks and gluinos have at least two large-E_T jets associated with large $\not\!\!E_T$. Furthermore, the jet multiplicity tends to be larger for events with gluino than with squark. The final state with lepton(s) is possible due to leptonic decays of the $\tilde{\chi}_1^\pm$

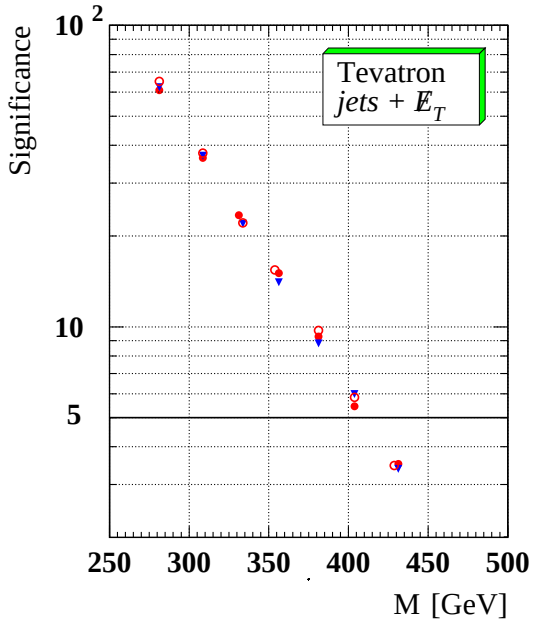

Figure 2: Significance as a function of $M_{\tilde{g}}$ ($M_{\tilde{q}} \simeq M_{\tilde{g}}$) for $\tan\beta = 3$ (filled circles), 10 (down triangles), and 30 (open circles) in jets + $\not\!\!E_T$ channel (15 fb^{-1}) at the Tevatron [20].

and/or $\tilde{\chi}_2^0$. The branching ratio to the final state with two or more leptons strongly depends on the value of $\tan\beta$. This leads us to look for SUSY events with final states of from jets + $\not\!\!E_T$ and 1ℓ + jets + $\not\!\!E_T$ ($\ell = e$ or μ) [20]. We restrict the parameter space so that lighter third generation squarks ($\tilde{b}_1$ and $\tilde{t}_1$) remain heavier than the $\tilde{\chi}_1^{\pm}$ and the $\tilde{\chi}_2^0$.

In the jets + $\not\!\!E_T$ channel, for example, an optimization of cuts could be made on N_j, $\not\!\!E_T$, and M_{S_2} ($\equiv \not\!\!E_T + E_T^{j_1} + E_T^{j_2}$) [20]. The final selection cuts are: (a) $N_j \geq 4$; (b) veto on isolated leptons (e or μ) with $p_T > 15$ GeV/c; (c) $\not\!\!E_T > 100$ GeV; (d) $\Delta\phi_{j\not\!\!E_T} > 30°$; (e) $M_{S_2} > 350$ GeV. The SM background sizes are estimated to be 25 fb for $t\bar{t}$ events, 38 fb for W/Z + jets events, 1 fb for diboson process, and 9 fb for QCD events, totaling 73 fb. Figure 2 is the significance as a function of $M_{\tilde{g}}$ where $M_{\tilde{q}} \simeq M_{\tilde{g}}$ at $\tan\beta = 3$, 10, and 30 ($\mu > 0$ and $A_0 = 0$). The strongest reach in 5σ significance is 410 GeV/c^2 ($m_{1/2} \simeq 160$ GeV/c^2) for 15 fb^{-1}. There is no significant $\tan\beta$ dependence. This can be compared to 280 GeV/c^2 for 100 pb^{-1}, 360 GeV/c^2 for 2 fb^{-1}, and 440 GeV/c^2 for 30 fb^{-1}. This channel has huge QCD background events, so that Trigger B1 will play a key role to minimize systematic uncertainty in understanding the size of the QCD events.

In the 1ℓ + jets + $\not\!\!E_T$ channel, the gluino mass limits are less stringent than those in the jets + $\not\!\!E_T$ channel [20], except for smaller m_0 values. It will be essential to combine limits from the two channels to maximize the sensitivity in Run II.

Table 1: Discovery reaches on $M_{\tilde{b}_1}$ and $M_{\tilde{t}_1}$ expected in Run II [24]. The Run I limits are after taking into account LEP2 limits on $M_{\tilde{\chi}_1^0}$, $M_{\tilde{\ell}}$, and $M_{\tilde{\chi}_1^\pm}$. In Run II, $\ell bj\not{E}_T$ and $cc\not{E}_T$ final states will be explored by Trigger B2.

Decay ($Br = 100\%$)	Subsequent Decay	Final State of $\tilde{b}_1\bar{\tilde{b}}_1$ or $\tilde{t}_1\bar{\tilde{t}}_1$	Discovery Reach in $M_{\tilde{t}_1}$ or $M_{\tilde{b}_1}$ @20 fb^{-1}	(Run I)
$\tilde{b}_1 \to b\tilde{\chi}_1^0$		$bb\not{E}_T$	260 GeV/c^2	(146 GeV/c^2 [26])
$\tilde{t}_1 \to c\tilde{\chi}_1^0$		$cc\not{E}_T$	220 GeV/c^2	(116 GeV/c^2 [26])
$\tilde{t}_1 \to bl\tilde{\nu}$	$\tilde{\nu} \to \nu\tilde{\chi}_1^0$	$\ell^+\ell^- b\not{E}_T$	240 GeV/c^2	(140 GeV/c^2 [28])
$\tilde{t}_1 \to bl\nu\tilde{\chi}_1^0$		$\ell^+\ell^- b\not{E}_T$	-	(129 GeV/c^2 [28])
$\tilde{t}_1 \to b\tilde{\chi}_1^\pm$	$\tilde{\chi}_1^\pm \to W^{(*)}\tilde{\chi}_1^0$	$\ell bj\not{E}_T$ and $\ell^+\ell^- j\not{E}_T$	210 GeV/c^2	(-)
$\tilde{t}_1 \to bW\tilde{\chi}_1^0$		$\ell bj\not{E}_T$	190 GeV/c^2	(-)

It should be noted that the DØ and CDF analyses of the jets + $\not{E}_T$ channel within the mSUGRA framework ($A_0 = 0$) in Run I were limited to $\tan\beta = 3$, $\mu < 0$ [21, 22]. The stringent lower limit on the gluino mass at 95% C.L. is 300 GeV/c^2 ($m_{1/2} \simeq$ 130 GeV/c^2) for $\tan\beta = 3$ and $\mu < 0$ if $M_{\tilde{q}} = M_{\tilde{g}}$ [22]. The DØ analysis of the $1e$ + jets + $\not{E}_T$ channel in Run I was also limited to $\tan\beta = 3$, $\mu < 0$ [23] and the gluino mass limit was less stringent than those in the jets + $\not{E}_T$ channel.

3.1.3 Stop and Sbottom Production

A large mixing angle $\theta_{\tilde{t}}$ between the superpartners of the left-chiral and the right-chiral stop quarks, $\tilde{t}_L$ and $\tilde{t}_R$ respectively, form two squark mass eigenstates where $M_{\tilde{t}_1} < M_{\tilde{t}_2}$. The $\tilde{t}_1$ could substantially be lighter than other squarks. mSUGRA with smaller m_0 and/or larger $|A_0|$ would have a light stop in their spectrum. In contrast, lighter sbottom ($\tilde{b}_1$) can appear only at small m_0 and small $m_{1/2}$ in the mSUGRA models. In addition, they are always accompanied by light stops, except $\tan\beta > 20$ and $\mu < 0$.

For general studies, we simply assume either $\tilde{b}_1$ or $\tilde{t}_1$ is the lightest squark. A comprehensive study on prospects of those searches can be found in Refs. [24, 4]. Decays studied for the $\tilde{t}_1$ or $\tilde{b}_1$ in Run II are: (i) $\tilde{b}_1 \to b\tilde{\chi}_1^0$, (ii) $\tilde{t}_1 \to c\tilde{\chi}_1^0$, (iii) $\tilde{t}_1 \to bl\tilde{\nu}(b\tilde{\ell}\nu)$, (iv) $\tilde{t}_1 \to b\tilde{\chi}_1^\pm$, followed by $\tilde{\chi}_1^\pm \to W^{(*)}\tilde{\chi}_1^0 \to \ell\nu\tilde{\chi}_1^0$, (v) $\tilde{t}_1 \to bW\tilde{\chi}_1^0$.

Table 1 is a summary of the maximum sensitivity in the searches. In Run II, we should also consider the case where the branching ratio for $\tilde{t}_1 \to b\tilde{\chi}_1^{\pm(*)} \to b\tilde{\tau}\nu$ is nearly 100%. Trigger A should enhance the sensitivity of the search. It should be noted that the above studies are based on bino-like LSP. For higgsino-like LSP, the search strategy needs to be modified and its prospects can be found in Ref. [24].

The LEP limits on $\tilde{\chi}_1^\pm$ and $\tilde{\ell}$ masses [25] leave the decays of (a) $\tilde{b}_1 \to b\tilde{\chi}_1^0$ [26, 27], (b) $\tilde{t}_1 \to c\tilde{\chi}_1^0$ [26], (c) $\tilde{t}_1 \to b\ell\tilde{\nu}$ (three-body decay, $M_{\tilde{\nu}} = M_W$) $\to b\ell\nu\tilde{\chi}_1^0$ [28], and (d) $\tilde{t}_1 \to b\ell\nu\tilde{\chi}_1^0$ (four-body decay, $M_{\tilde{\nu}} = M_{\tilde{t}_1} - M_b$) [28] in Run I. A summary of the mass limits is also provided in Table 1. For cases (c) and (d), we simply assumed the three final states of $be\nu\tilde{\chi}_1^0$, $b\mu\tilde{\nu}\tilde{\chi}_1^0$, and $b\tau\nu\tilde{\chi}_1^0$ have the same branching ratio of 33.3%.

Table 2: Discovery reach (5σ significance) on SUSY mass for various NLSP scenarios in minimal GMSB models [5]. In $c\tau$ column, "p" and "d" indicate prompt and displaced decays of NLSP, respectively, while "ll" for long-lived NLSP. γ_d indicates a displaced photon. δ_{im} indicates an impact parameter.

NLSP	Decay Mode	$c\tau$	Prod.	Key Final State(s)	Discovery Reach @30 fb^{-1}
Bino $\tilde{\chi}_1^0$	$\gamma + \tilde{G}$	p	all	$\gamma\gamma \not\!\!E_T + X$	340 GeV/c^2 ($\tilde{\chi}_1^\pm$)
		d	all	$\gamma_d jj \not\!\!E_T$ or $\gamma\gamma \not\!\!E_T + X$	300 GeV/c^2 ($\tilde{\chi}_1^\pm$) ($c\tau$ = 50 cm)
Higgsino $\tilde{\chi}_1^0$	$(h, Z, \gamma) + \tilde{G}$	p	all	$(hh, h\gamma, hZ, Z\gamma, ZZ, \gamma\gamma) \not\!\!E_T + X$	220 GeV/c^2 ($\tilde{\chi}_1^\pm$)
		d	all	$\delta_{ip} < 0$ for $h \to bb$, $Z \to \ell^+\ell^-$	–
		d	all	$\gamma_d + X$	–
$\tilde{\tau}$	$\tau + \tilde{G}$	p	all	$\ell\ell\ell j \not\!\!E_T$, $\ell^\pm\ell^\pm jj \not\!\!E_T$, $\tau_h\tau_h \not\!\!E_T$	230 GeV/c^2 ($\tilde{\chi}_1^\pm$) 120 GeV/c^2 ($\tilde{\tau}_1$)
		ll	all	$\mu(dE/dx) + \ell\ell(M_{\ell\ell} > 150$ GeV/$c^2)$	420 GeV/c^2 ($\tilde{\chi}_1^\pm$) 210 GeV/c^2 ($\tilde{\tau}$)
		ll	all	$\mu(dE/dx) + X$	180 GeV/c^2 ($\tilde{\tau}$)
		ll	all	$\mu(dE/dx$+TOF$) + X$	210 GeV/c^2 ($\tilde{\tau}$)
$\tilde{\ell}$ co-NLSP	$\ell + \tilde{G}$	p	all	$\ell\ell\ell j \not\!\!E_T$	360 GeV/c^2 ($\tilde{\chi}_1^\pm$) 160 GeV/c^2 ($\tilde{\ell}$)
		d	all	$\ell\ell + dE/dx$	480 GeV/c^2 ($\tilde{\chi}_1^\pm$) 206 GeV/c^2 ($\tilde{\ell}$)
$\tilde{t}_1$	$(c, bW) + \tilde{G}$	p	$\tilde{t}_1\tilde{t}_1$	$cc \not\!\!E_T$ or $\ell + jets + \not\!\!E_T$	175 GeV/c^2 ($\tilde{t}_1$)

3.2 Testing GMSB

The GMSB models are generally distinguished by the presence of a nearly massless Goldstino ($\tilde{G}$) as the LSP. The next-to-lightest SUSY particle (NLSP) decays to its partner and the $\tilde{G}$. Depending on the SUSY breaking scale ($\sqrt{F}$) , these decays occur promptly ($\sqrt{F} \lesssim$ a few 100 TeV) or on a scale comparable to the size of a collider detector (a few 100 TeV $\lesssim \sqrt{F} \lesssim$ a few 1000 TeV). For $\sqrt{F}$ much larger than a few 1000 TeV, the NLSP decay takes place well outside a collider detector and are not directly relevant to accelerator physics. Thus we consider a systematic analysis based on a classification in terms of the identity of the NLSP and its decay length within the minimal GMSB models. The models can be specified in terms of six parameters [5]: N_m (the number of generations of messenger fields), M_m (an overall SUSY mass for the messengers), Λ (the effective visible sector SUSY breaking parameter $= F_S/M_m$), C_G (the ratio of the messenger sector SUSY breaking order parameter to the intrinsic SUSY breaking order parameter, F/F_S, controlling the coupling to the Goldstino), in addition to $\tan\beta$ and sign(μ). The NLSP decay length scales like C_G^2.

The NLSP can be bino-like $\tilde{\chi}_1^0$, higgsino-like $\tilde{\chi}_1^0$, $\tilde{\tau}_1$, $\tilde{\ell}$, or $\tilde{q}$ (likely $\tilde{t}_1$) in minimal GMSB. We here choose two scenarios, bino-like $\tilde{\chi}_1^0$ and $\tilde{\tau}_1$, because the signatures define special detector performance at CDF and DØ other than in Section 3.1. A summary of discovery reaches for various NLSP scenarios is given in Table 2.

3.2.1 Bino-like Neutralino NLSP

For $\sqrt{F}$ greater than a few 1000 TeV, the $\tilde{\chi}_1^0 \to \tilde{G} + \gamma$ decay takes place outside a collider detector. In this case, $\tilde{\chi}_1^0$ is essentially stable on the scale of the experiment and escapes as missing energy. If $\sqrt{F}$ is less than that, however, the $\tilde{\chi}_1^0$ decay takes place within the detector. Thus, two hard photons and large $\not\!\!E_T$ would be observed in all final states of pair produced SUSY particles with cascade decays through the $\tilde{\chi}_1^0$ decay. There is essentially no SM background.

For a representative study for $\gamma\gamma\not\!\!E_T + X$, models are chosen with $N_m = 1$, $M_m/\Lambda = 2$, $\tan\beta = 2.5$, and $\mu > 0$ [5]. Here $\gamma\gamma$ are either prompt or displaced photons. In the models, the cross-section for $\tilde{\chi}\tilde{\chi}$ ($\tilde{\chi}_1^+\tilde{\chi}_1^-$ and $\tilde{\chi}_1^\pm\tilde{\chi}_2^0$) production is the largest. Thus, the $\tilde{\chi}_1^\pm$ is probably the best figure of merit for the discovery reach.

For prompt photon, CDF and DØ collaborations studied the final state with different kinematical cuts [29], but found similar 5σ discovery reach (with 30 fb^{-1}) in $M_{\tilde{\chi}_1^\pm}$: 330 GeV/c^2 for CDF and 340 GeV/c^2 for DØ [5].

For a displaced photon, the DØ detector can reconstruct the electromagnetic (EM) shower developments in the EM calorimeters to point back to the beam line to measure the distance of closest approach (d_{ca}) to the beam axis [5]. The analysis requires at least one photon with $d_{ca} > 5$ cm in the final state of $\gamma_d jj\not\!\!E_T$. Here γ_d indicates a displace photon. For $\Lambda = 100$ TeV ($M_{\tilde{\chi}_1^\pm} \simeq 250$ GeV/c^2, $M_{\tilde{\chi}_1^0} \simeq 130$ GeV/c^2), the probability that a photon has $d_{ca} > 5$ cm is about 40% or better for $c\tau \lesssim 100$ cm. The discovery reach in the $\tilde{\chi}_1^\pm$ mass ranges from 310 GeV/c^2 to 280 GeV/c^2 between $c\tau =$ 0 and 100 cm. On the other hand, CDF will measure the photon's arrival time on the EM calorimeter to distinguish from prompt photon or cosmic-ray induced photon [30].

3.2.2 Stau NLSP

The models are $N_m = 2$, $M_m/\Lambda = 3$, $\tan\beta = 15$, $\mu > 0$ with Λ allowed to vary [5]: the $\tilde{\tau}_1$ is lighter than $\tilde{\chi}_1^0$, but $M_{\tilde{\tau}_1} \sim 0.5 M_{\tilde{\chi}_1^\pm}$. $M_{\tilde{\ell}_R} - M_{\tilde{\tau}_1}$ is greater than a few GeV/c^2 for all points. The $\tilde{\chi}_1^+\tilde{\chi}_1^-$ and $\tilde{\chi}_1^\pm\tilde{\chi}_2^0$ production is dominant for $M_{\tilde{\chi}_1^\pm} \lesssim 350$ GeV/c^2 and the $\tilde{\tau}_1\tilde{\tau}_1$ production becomes dominant for heavier $\tilde{\chi}_1^\pm$.

If $\tilde{\tau}_1$ is short-lived and decays in the vicinity of the production vertex, the $\tilde{\chi}\tilde{\chi}$ production, followed by the cascade decays, will arise in the final states of $\ell\ell\ell j\not\!\!E_T$ and $\ell^\pm\ell^\pm jj\not\!\!E_T$. They are studied by DØ, while CDF investigates the $\tau_h\tau_h\not\!\!E_T$ final state from $\tilde{\tau}_1 \to \tau\tilde{G}$. With 30 fb^{-1}, both analyses have the discovery reach of 230 (120) GeV/c^2 in $M_{\tilde{\chi}_1^\pm\ (\tilde{\tau}_1)}$.

For long-lived $\tilde{\tau}_1$, we search for events containing at least one μ-like track with a large dE/dx in its tracking system. The DØ analysis choose the final state including two leptons with $M_{\ell\ell} > 50$ GeV/c^2 and is sensitive for the $\tilde{\chi}\tilde{\chi}$ production. With 30 fb^{-1}, the discovery reaches in $M_{\tilde{\chi}_1^\pm}$ ($M_{\tilde{\tau}_1}$) are 420 (210) GeV/c^2.

The CDF detector includes a new time-of-flight (TOF) system. With a timing resolution of 100 ps, we could require 4σ separation (at 400 ps), which is $\beta\gamma < 2.26$ (or $p < 235$ GeV/c^2). This should be compared to $\beta\gamma < 0.85$ using the dE/dx technique

alone. With 30 fb^{-1}, the discovery reaches in $M_{\tilde{\tau}_1}$ are 180 GeV/c^2 with dE/dx and 210 GeV/c^2 with dE/dx plus TOF.

It should be noted that the same technique (dE/dx, TOF) can be used [6] to test Anomaly-mediated SUSY Breaking (AMSB) models [31] where the $\tilde{\chi}_1^{\pm}$ is long-lived because of a very small mass difference between $\tilde{\chi}_1^{\pm}$ and $\tilde{\chi}_1^0$.

3.3 Summary

The ultimate limit for the SUSY mass reach of a hadron collider, resulting from the distribution function of the constituent quarks and gluons, is $\sim$ 25% of its collider energy. Thus the Tevatron approaches its limit below 450 GeV/c^2 (about 50% $\sqrt{s}$) in the discovery of the SUSY particles. This would be similar to the CERN Super Proton Synchrotron (S$p\overline{p}$S) that approached its limit in the discovery of the W and Z bosons.

4 Detection of $B_s \to \mu^+\mu^-$

We consider now the possibility of detecting the decay $B_s \to \mu^+\mu^-$ by the CDF and DØ detectors at the Tevatron in Run II [32]. Both detectors have been upgraded with excellent tracking and muon detector systems [33]. The dimuon trigger is the key to collect the $B_s \to \mu^+\mu^-$ decays.

This process is particularly interesting for several reasons: The SM branching ratio is quite small, *i.e.*, $Br[B_s \to \mu^+\mu^-]_{\rm SM} = 3.5 \times 10^{-9}$ [33]. The SUSY contribution [34, 35, 36, 37, 38, 39, 40] has terms that grow as $\tan^6\beta$ and thus can become quite large for large $\tan\beta$. Finally, as we shall show below, the two collider detectors will be sensitive to this decay for $\tan\beta \gtrsim 30$ in Run II.

In order to estimate the limits on $Br[B_s \to \mu^+\mu^-]$ detection, we use the 95% C.L. limit on $Br[B_s \to \mu^+\mu^-]$ published by CDF[41]. Thus our discussion is based on the CDF detector, although both CDF and DØ detectors should have a similar performance.

In the Run I analysis, CDF observed one candidate that was consistent with $B_s \to \mu^+\mu^-$ with an estimate of 0.9 background (BG) events in 98 pb^{-1} [41]. The primary Run-I selection variables and cut values were $c\tau \equiv L_{xy}M_B/p_T^{\mu\mu} > 100$ μm, $I \equiv p_T^{\mu\mu}/[p_T^{\mu\mu} + \Sigma p_T] > 0.75$ for the muon pair, and $\Delta\Phi < 0.1$ rad. Here, L_{xy} is the transverse decay length; $p_T^{\mu\mu}$ is the transverse momentum of the dimuon system. Σp_T is the scalar sum of the transverse momenta of all tracks, excluding the muon candidates, within a cone of $\Delta R \equiv \sqrt{(\Delta\eta)^2 + (\Delta\phi)^2} = 1$ around the momentum vector of the muon pair. The z coordinate of each track along the beam line [42] must be within 5 cm of the primary vertex. $\Delta\Phi$ is an opening azimuthal angle between $p_T^{\mu\mu}$ and the vector pointing from the primary vertex to the secondary vertex (the reconstructed B-meson decay position). As a conservative estimate, CDF took the one event as signal to calculate 95% C.L. limit of signal events ($N_1^{95\%} \equiv 5.06$ events [41]) and had set a limit of $Br < 2.6 \times 10^{-6}$. In the analysis, the selection efficiency (ϵ) for signal events and the rejection power ($\mathcal{R}$) for background events (pass a baseline selection [41]) are

estimated to be $\epsilon_1 = 0.45$ and $\mathcal{R}_1 = 440$ by using a sample of like-sign dimuon events ($5 < M_{\mu\mu} < 6$ GeV/c^2).

In Run II, a dimuon trigger in Ref. [33] will improve the acceptance for signal events by a factor of 2.8. The trigger will soon be tested using the Run IIa (2 fb^{-1}) data. This will allow us to modify the trigger design for the higher luminosity expected in Run IIb (15 fb^{-1}). In this paper, we assume that the dimuon trigger can be designed by maintaining the acceptance for signal events. We expect to improve the acceptance for signal events by a factor of 2.8 [33]. If we assume the factor 2.8 to be the same for BG events, then we would observe 51 (386) events in 2 (15) fb^{-1} with the same cuts as in Run I. Therefore, CDF has to require a set of tighter cuts to obtain the best possible upper limit.

Two types of backgrounds must be taken into account: (i) non-b backgrounds coming from the primary vertex; (ii) b background events, such as the gluon-spliting $b\overline{b}$ events.

One way to reduce prompt background is to require a minimum decay length L_{xy}. However, two tracks can appear to form a secondary vertex if one of two tracks originates from the primary vertex and the other has an impact parameter (δ). Therefore, the requirement of a minimal impact parameter of individual tracks can further clean up the sample. It has been shown for example, in the Run-I analysis for $B^0 \to K^{0*}\mu^+\mu^-$ events [43], that a tight impact parameter cut on significance for individual track ($\delta/\sigma_\delta > 2$) significantly improve the background rejection even with $L_{xy} > 100$ μm. One has then $\epsilon \sim \epsilon_1 \times 0.43$ and $\mathcal{R} \sim \mathcal{R}_1 \times 190$. Thus a higher track impact parameter is necessary to reduce the non-b backgrounds. We would expect larger reduction with good efficiency even after the L_{xy} cut. The silicon vertex detector (SVX-II) will provide us much better reduction for the non-b background than Run I.

The most severe background in Run II will be the two muons from gluon-spliting $b\overline{b}$ events. Since both particles are b quarks, the impact parameter does not help. Both b and $\overline{b}$ also go in the same direction, so that cut on L_{xy} does not help either. However, $\Delta\Phi$ is still useful to remove the background events. Furthermore, in Run II, we can use $\Delta\Theta$ in r-z view since we have z-strips in SVX-II.

There is some room to improve the isolation cut. We can form a new isolation parameter by only using the tracks with large impact parameter. This new isolation cut will work to reject the $b\overline{b}$ rather than non-b background. Furthermore, we can search for tracks with large impact parameter on the opposite side of the dimuon candidates to make sure that the b and $\overline{b}$ go to the opposite side.

Therefore, CDF could improve the BG rejection by a factor of 200-400 with further reduction of the signal efficiency by a factor of 2-3. Based on these facts, we now consider two cases to evaluate Run II limits as a function of luminosity.

In the first case (Case A), we naively assume new tighter cuts in Run II, described above, will gain additional BG rejection power of 450 for additional efficiency of 0.45, or $\mathcal{R}_2 = 450^{0.45/\epsilon_2}$. This gives us

$$\frac{\epsilon_2}{\epsilon_1} = \frac{1}{1 + \log(\mathcal{R}_2/\mathcal{R}_1)/\log(450)} \quad (1)$$

If we could optimize the BG rejection in Run IIa (2 fb^{-1}) to be $\mathcal{R}_2 \approx 51\mathcal{R}_1$ with

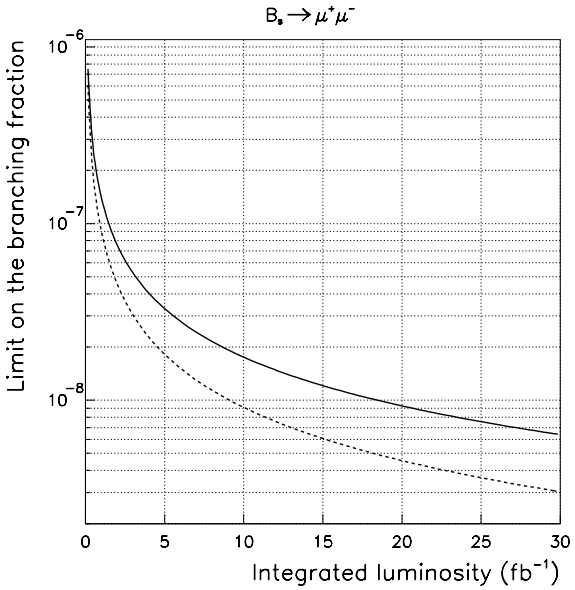

Figure 3: Illustrated 95% C.L. limits on the branching ratio for $B_s \to \mu^+\mu^-$ at CDF in Run II as a function of integrated luminosity [32]. Solid (Case A) and dashed (Case B) curves are based on different assumptions on the signal selection efficiency and the background rejection power. See the text for details.

$\epsilon_2 \approx 0.61\epsilon_1$ (from Eq. 1), then we would expect one BG event in 2 fb^{-1}. Thus, with an assumption of the same size of the total systematic uncertainty in Run II as in Run I, we can extrapolate the 95% C.L. limit to be $Br < 7.7 \times 10^{-8}$ for 2 fb^{-1} using $N_1^{95\%}$.

In the second case (Case B), we simply assume the Run-II background rejection could be improved (without loosing the signal efficiency) to keep the expected BG events in 2 fb^{-1} at the level of Run I (*i.e.*, 0.9 events). If we would observe one event in 2 fb^{-1}, then we could set the limits by scaling the Run-I Br limit down by the luminosity (2000 pb^{-1}/98 pb^{-1}) and the acceptance by (2.8/1.0). Thus we obtain $Br < 4.6 \times 10^{-8}$. This would certainly be the optimistic scenario, but it would be a goal of this analysis in Run IIa. Here, the systematic uncertainty in Run II is assumed to be the same as in Run I.

We repeat the same argument for different luminosities. Figure 3 shows 95% C.L. limits on $Br[B_s \to \mu^+\mu^-]$ at CDF in Run II as a function of integrated luminosity for Cases A and B. For 15 fb^{-1} in case A, CDF would be sensitive to $Br > 1.2 \times 10^{-8}$ and the combined CDF and DØ data (30 fb^{-1}) would be sensitive to $Br > 6.5 \times 10^{-9}$.

We examine first the parameter region for the mSUGRA model that would be accessible to CDF or DØ at Run II with 15 fb^{-1} of data. Figure 4(left) shows the $Br[B_s \to \mu^+\mu^-]$ as a function of $m_{1/2}$ for $A_0 = 0$, $m_0 = 300$ GeV. One sees that with a sensitivity of $Br[B_s \to \mu^+\mu^-] > 1.2 \times 10^{-8}$ for 15 fb^{-1}, the Tevatron Run II can probe the $B_s \to \mu^+\mu^-$ decay for $\tan\beta > 30$. Further, a search for this decay would sample much higher regions of $m_{1/2}$ than a direct search at Run II for SUSY particles which is restricted to $m_{1/2} < 250$ GeV [13]. As m_0 increases, the branching ratio goes down.

However, this dependence becomes less significant for large $m_{1/2}$, where m_0 as large as 800 GeV can be sampled for large $m_{1/2}$.

In Figure 4(right) the contours of $Br[B_s \to \mu^+\mu^-]$ are plotted in the m_0-$m_{1/2}$ plane for $\tan\beta = 50$, $A_0 = 0$. Also see Figure 1. We combine now this result with the other experimental constraints. Thus the shaded region to the left is ruled out by the $b \to s\gamma$ constraint, and the shaded region on the right hand side is disallowed if $a_\mu^{\rm SUGRA} > 11 \times 10^{-10}$. The narrow shaded band in the middle is allowed by the dark matter constraint. We note that independent of whether the astronomically observed dark matter is SUSY in origin, the dark matter allowed region for mSUGRA cannot significantly deviate from this shaded region, for below the narrow shaded band, the stau would be lighter than the neutralino (leading to charged dark matter), while above the band, mSUGRA would predict more neutralino dark matter than is observed.

Using our estimate that $Br > 1.2 \times 10^{-8}$ can be observed with 15 fb^{-1}, we see that almost the entire parameter space allowed by the $a_\mu < 11 \times 10^{-10}$ constraint can be probed in Run II for $\tan\beta = 50$. Note that an observed $Br[B_s \to \mu^+\mu^-] > 7 \times 10^{-8}$, possible with only 2 fb^{-1}(see Figure 3), would be sufficient to rule out the mSUGRA model for $\tan\beta \leq 50$. In Figure 4(right) we also show the expected dark matter detector cross section for Milky Way dark matter (the short solid lines). For $\tan\beta = 40$ and $A_0 = 0$, we see about half the parameter space can be scanned by the CDF detector (and the whole parameter space with 30 fb^{-1} if a similar analysis holds for the DØ detector). We note, further, that if $A_0 = 0$, a simultaneous measurement of both $Br[B_s \to \mu^+\mu^-]$ and a_μ would essentially determine the mSUGRA parameters, as the m_0 allowed region at fixed $m_{1/2}$ is very narrow due to the dark matter constraint. The effect of varying A_0 is also discussed in Ref. [32].

In Figures 4(right), we have also drawn lines for various light Higgs masses (vertical dotted lines). A measurement of $B_s \to \mu^+\mu^-$, a_μ and m_h would then effectively determine the parameters of mSUGRA for $\mu > 0$ by requiring that they intersect with the dark matter allowed band at a point. (If no choice of parameters allowed this, mSUGRA would be ruled out.) The Tevatron Run II should be able to either rule out a Higgs mass or give evidence for its existence at the 3σ level over the entire allowed mass range of SUSY light Higgs masses. Alternatively, the LHC's determination of m_h or the gluino mass (to determine $m_{1/2}$) would fix the parameters of mSUGRA.

Thus if a_μ increases, the bound moves downward, encroaching further on the allowed part of the parameter space, and a value of $a_\mu \gtrsim 50 \times 10^{-10}$ would eliminate the mSUGRA model [44]. However, if a_μ decreases significantly (but is still positive), the mSUGRA model would predict a heavy SUSY particle spectra closer to the TeV region, having significant effects on accelerator and dark matter detection physics. An accurate determination of a_μ corresponds to a line from upper left to lower right (or more precisely a band when errors are included) running parallel to the $a_\mu < 11 \times 10^{-10}$ boundary, and cutting through the allowed dark matter band which runs from lower left to upper right. Thus, these two experiments are complementary for determining the mSUGRA parameters.

It is also pointed out that the $B_s \to \mu^+\mu^-$ decay is very powerful in testing the SUSY breaking mechanism [45]. If the $B_s \to \mu^+\mu^-$ decay is observed with $Br > 10^{-8}$, the Tevatron could exclude (i) GMSB models (with $\tan\beta < 40$ and lower N_m) and

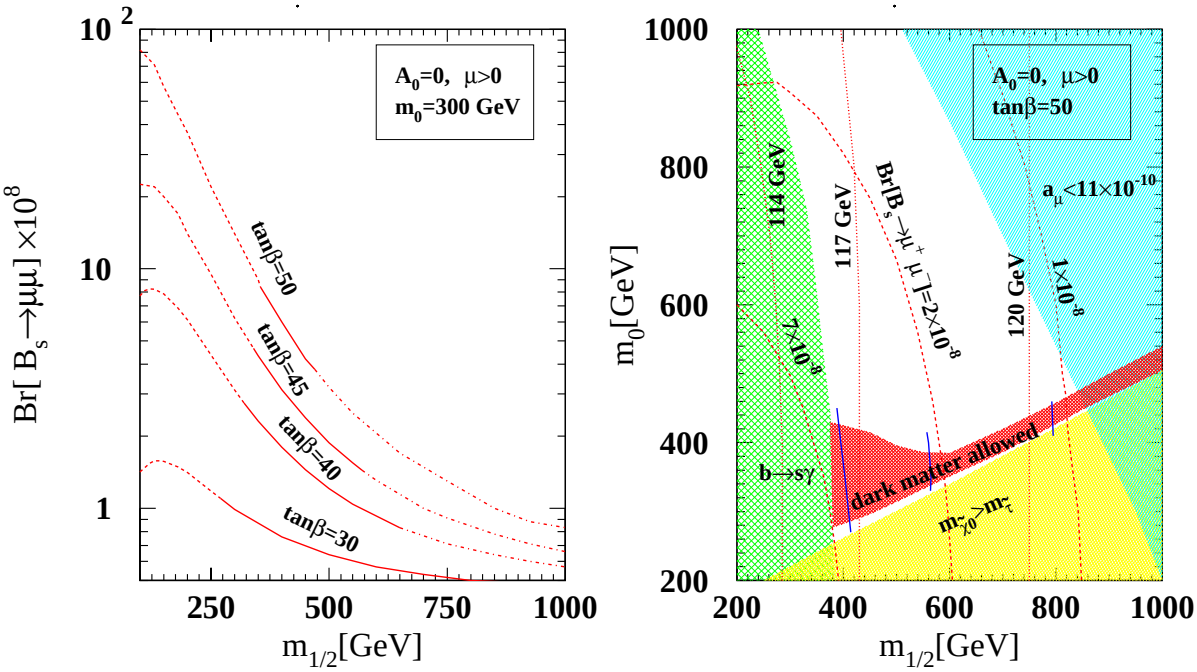

Figure 4: Branching ratio for $B_s \to \mu^+\mu^-$ in mSUGRA models [32]. On the left plot, $Br[B_s \to \mu^+\mu^-]$ is shown as a function of $m_{1/2}$ for various $\tan\beta$ values, where dashed and dash-dotted lines are to indicate the models are excluded via constraints on $Br[b \to s\gamma]$ and $m_{\tilde{\tau}} > m_{\tilde{\chi}_1^0}$, respectively. On the right plot, three dashed lines from left to right in the m_0-$m_{1/2}$ plane indicate $Br = 7 \times 10^{-8}$, 2×10^{-8}, 1×10^{-8}, respectively, for $\tan\beta = 50$. The three short solid lines indicate the $\sigma_{\tilde{\chi}_1^0 - p}$ values (from left: 0.05 $\times 10^{-6}$ pb, 0.004 $\times 10^{-6}$ pb, 0.002 $\times 10^{-6}$ pb). The vertical dotted lines label Higgs masses.

(ii) minimal AMSB models.

Interestingly, unlike the R parity conserving models, the SUSY contribution to $B_s \to \mu^+\mu^-$ can occur at the tree level in the R parity violation models. The $Br[B_s \to \mu^+\mu^-]$ can be large for both small and large $\tan\beta$. We, for example, consider lepton violating terms [46], and so we set λ'' to zero (to prevent rapid proton decay). In Ref. [32], the branching ratio of 10^{-7} (feasible with 2 fb^{-1}) could be sensitive upto $m_{1/2} \lesssim 1000$ (750) GeV/c^2 for $m_0 = 300$ (500) GeV/c^2.

5 Conclusion

We have investigated the prospects for studying SUSY parameter space in Run II of the Fermilab Tevatron. Two complementary observables (especially in SUGRA models) are of great interest [15]: trilepton final state as production of charginos and neutralinos for lower $\tan\beta$ values and the rare decay mode $B_s \to \mu^+\mu^-$ for large $\tan\beta$ values.

Especially, the $B_s \to \mu^+\mu^-$ decay is an important process for SUSY searches, as the Standard Model prediction of the branching ratio is quite small (3.5×10^{-9}), and the SUSY contribution increases for large $\tan\beta$ as $\tan^6\beta$. We find that a $Br > 1.2 \times 10^{-8}$

for 15 fb^{-1} can be probed by each collider detector in Run II. (This is nearly a factor of 100 improvement over the Run I bound.) For the mSUGRA model, the above sensitivity implies that Run II could probe a region of parameter space for $\tan\beta > 30$, a region which could not be probed by a direct search at Run II. A large branching ratio, *i.e.*, $> 7 \times 10^{-8} (14 \times 10^{-8})$ would be sufficient to eliminate the mSUGRA model for $\tan\beta \leq 50(55)$ if one combined the expectations for $B_s \to \mu^+\mu^-$ for mSUGRA with other experimental bounds on the parameter space.

Acknowledgments

I wish to thank the organizers of the SUSY02 conference for their excellent hospitality. I should thank CDF and DØ collaborations to provide valuable information and discussions.

References

[1] CDF II Collaboration, Fermilab-Pub-96/390-E (1996).

[2] DØ II Collaboration, Fermilab-Pub-96/357-E (1996).

[3] P. Langacker, Proceedinsg of the APS/DPF/DPB Summer Study on the Future of Particle Physics (Snowmass 2001), ed. R. Davidson and C. Quigg, arXiv: `hep-ph/0110129` .

[4] V. Barger *et al.*, arXiv: `hep-ph/0003154`.

[5] R. Culbertson *et al.*, arXiv: `hep-ph/0008070`.

[6] S. Ambrosanio *et al.*, arXiv: `hep-ph/0006162`.

[7] M. Carena *et al.*, arXiv: `hep-ph/0010338`.

[8] For a review of the SUSY searches at CDF and DØ, see M. Carena *et al.*, arXiv: `hep-ex/9712022`.

[9] A. H. Chamseddine, R. Arnowitt, and P. Nath, Phys. Rev. Lett. **49**, 970 (1982).

[10] R. Barbieri, S. Ferrara, and C. A. Savoy, Phys. Lett. B**119**, 343 (1982); L. J. Hall, J. Lykken, and S. Weinberg, Phys. Rev. D**27**, 2359 (1983); P. Nath, R. Arnowitt, and A. H. Chamseddine, Nucl. Phys. B**227**, 121 (1983).

[11] T. Kamon, J. L. Lopez, P. McIntyre, and J. T. White, Phys. Rev. D**50**, 5676 (1994).

[12] H. Baer *et al.*, Phys. Rev. D**58**, 075008 (1998).

[13] V. Barger, C. Kao, and T. Li Phys. Lett. B**433**, 328 (1998); V. Barger and C. Kao, Phys. Rev. D**60**, 115015 (1999).

[14] K. Matchev and D. Pierce, Phys. Rev. D**60**, 075004 (1999); J. Lykken and K. Matchev, Phys. Rev. D**61**, 015001 (2000).

[15] A. Dedes, H. K. Dreiner, U. Nierste, and P. Richardson, arXiv:hep-ph/0207026.

[16] CDF Collaboration, F. Abe *et al.*, Phys. Rev. Lett. **80**, 5280 (1998).

[17] DØ Collaboration, B. Abbott *et al.*, Phys. Rev. Lett. **80**, 1591 (1998). The upper limit on $\sigma \cdot Br$ is given for a single trilepton mode. To compare with the CDF result [16], the DØ limit should be scaled up by 4.

[18] T. Kamon (CDF Collaboration), Fermilab-Conf-98/246-E, Proceedings of the *Richard Arnowitt Fest*, Texas A&M University, College Station, TX, April 5-8, 1998.

[19] For example, $M_{\tilde{q}} - M_{\tilde{\chi}_1^\pm} \gtrsim 250$ GeV/c^2 and $M_{\tilde{\chi}_1^\pm} - M_{\tilde{\chi}_1^0} \gtrsim 45$ GeV/c^2 when $M_{\tilde{\chi}_1^\pm} > 100$ GeV/c^2.

[20] V. Krutelyov *et al.*, Phys. Lett. B**505**, 161 (2001).

[21] DØ Collaboration, B. Abbott *et al.*, Phys. Rev. Lett. **83**, 4937 (1999).

[22] CDF Collaboration, T. Affolder *et al.*, Phys. Rev. Lett. **88**, 041801 (2002).

[23] DØ Collaboration, V. M. Abazov *et al.*, arXiv: `hep-ex/0205002`, submitted to Phys. Rev. D.

[24] R. Demina *et al.*, Phys. Rev. D**62**, 035011 (2000).

[25] LEP SUSY Working Group, ALEPH, DELPHI, L3 and OPAL Collaborations, LEPSUSYWG/01-03.1 (2001), LEPSUSYWG/02-01.1 (2002), LEPSUSYWG/02-02.1 (2002), `http://lepsusy.web.cern.ch/lepsusy/`.

[26] CDF Collaboration, F. Abe *et al.*, Phys. Rev. Lett. **84**, 5704 (2000).

[27] DØ Collaboration, B. Abbott *et al.*, Phys. Rev. D**60**, 031101 (1999).

[28] C. Pagliarone, CDF and DØ Collaborations, Proceedings of SUSY02 (2002).

[29] For the $\gamma\gamma \not\!\!E_T + X$ analysis with prompt photons, CDF uses $E_T^\gamma > 14$ GeV and $\not\!\!E_T > 40$ GeV, while DØ uses $E_T^\gamma > 20$ GeV and $\not\!\!E_T > 50$ GeV.

[30] CDF II Collaboration, Techinical Design Report for Run IIb Upgrade (2002).

[31] L. Randall and R. Sundrum, Nucl. Phys. B**557**, 79 (1999); G. F. Giudice, M. A. Luty, H. Murayama, and R. Rattazzi, JHEP 9812, 027 (1998); T. Gherghetta, G. F. Giudice, and J. D. Wells, Nucl. Phys. B**559**, 27 (1999).

[32] R. Arnowitt, B. Dutta, T. Kamon, and M. Tanaka, Phys. Lett. B**538**, 121 (2002).

[33] K. Anikeev *et al.*, arXiv: hep-ph/0201071.

[34] K. S. Babu and C. Kolda, Phys. Rev. Lett. **84**, 228 (2000).

[35] P. H. Chankowski and L. Slawianowska, Acta Phys. Polon. B **32**, 1895 (2001).

[36] C. Bobeth, T. Ewerth, F. Kruger, and J. Urban, Phys. Rev. D**64**, 074014 (2001).

[37] A. Dedes, H. K. Dreiner, and U. Nierste, Phys. Rev. Lett. **87**, 251804 (2001).

[38] G. Isidori and A. Retico, JHEP **0111**, 001 (2001).

[39] C. S. Huang and W. Liao, Phys. Rev. D**63** 11402 (2001); (E) D**64** 059902 (2001); arXiv: hep-ph/0201121.

[40] J. K. Mizukoshi, X. Tata, and Y. Wang, arXiv: hep-ph/0208078.

[41] CDF Collaboration, F. Abe *et al.*, Phys. Rev. D**57**, 3811 (1998).

[42] We use a coordinate system where θ and ϕ are the polar and azimuthal angles, respectively, with respect to the proton beam direction (z axis). The pseudorapidity (η) is defined as $-ln[\tan(\theta/2)]$. The transverse momentum of a particle is denoted as $p_T = p\ \sin\theta$.

[43] CDF Collaboration, T. Affolder *et al.*, Phys. Rev. Lett. **83**, 3378 (1999).

[44] R. Arnowitt, B. Dutta, B. Hu, and Y. Santoso, Phys. Lett. B**505**, 177 (2001).

[45] S. Baek, P. Ko, and W.-Y. Song, arXiv: hep-ph/0208112.

[46] J-H. Jang, J. K. Kim, and J. S. Lee, Phys. Rev. D**55**, 7296 (1997).